NIKHEF

NATIONAAL INSTITUUT VOOR KERNFYSICA EN HOGE-ENERGIEFYSICA

June 1983 NIKHEF-H/83-11

RADIATIVE CORRECTIONS TO TWO PHOTON PHYSICS

by

W.L. van Neerven and J.A.M. Vermaseren

NIKHEF-H

Amsterdam

Abstract:

We develop a method to calculate radiative corrections to two photon reactions of the type $e^+e^- \to e^+e^-X$ where X is an arbitrary final state. To illustrate this we take the example where X stands for a pointlike pseudoscalar. It will be shown that our method is an improvement on the standard way in adding real and virtual photon contributions to the (differential) cross-sections. This enables us to compute differential and total cross-sections to a very high precision and with a minimum of computer time which is not possible by using more conventional methods.

I. Introduction

In the last few years more and more data have been obtained from two photon processes. These reactions are very interesting because they give us an additional way to test the predictions of perturbative and nonperturbative QCD. In particular we want to mention that this reaction enables us to measure the photon structure function[1,2] if we look at a kinematical region where one photon is almost real and the other one is virtual. Other interesting observations can be made by looking at the resonances in the $\gamma\gamma$ channel. Besides the study of heavy flavours we expect that the above reaction may be an excellent mechanism to produce glue-ball states.

For all the two photon processes containing hadrons in the final state the pure QED reaction $e^+e^- \to e^+e^- \mu^+\mu^-$ serves as a calibration or a background. At this moment the data of this process[3] are in good agreement with the theoretical predictions obtained from the lowest order contributions[4]. This indicates that the radiative corrections[5,6] to this reaction are still smaller than the experimental errors. This situation may change if the accuracy of the experiments improves. Calculations of these higher order corrections show that the total cross-section will be changed by the order of one percent[5,6]. However, due to the intricacy of the numerical computation of the higher order contributions to these processes no reliable predictions are available for the single and double differential distributions. Therefore we want to investigate these radiative corrections more thoroughly than is done up to now. In particular it will be our goal to give an accurate prediction of the size of these differential distributions and the region of phasespace and energy where they are important. As a byproduct of this investigation we will develop a method which enables us to compute the sum of virtual and real photon graphs in a faster way than can be done by more conventional methods. The best way to do this is to start from the simplest example of a two photon process, i.e. wherein a (pseudo)scalar particle X of arbitrary mass is produced $e^+e^- \to e^+e^-X$. Once a suitable procedure has been found it is relatively straightforward to apply it to more realistic reactions like $e^+e^- \to e^+e^- \mu^+\mu^-$ or to other processes where $\mu^+\mu^-$ is replaced by an arbitrary final state.

In general the radiative corrections can be divided into four categories.

i) The corrections to the $e^{\pm}e^{\pm}\gamma$ vertices.
ii) photon exchanges between the (in) outgoing electrons and positrons,
iii) corrections to the leptons (e.g. $\mu^+\mu^-$) in the $\gamma\gamma$ final state,
iv) photon exchanges between the leptons in the $\gamma\gamma$ final state (e.g. $\mu^+\mu^-$) and the electron or the positron.

The (pseudo)scalar production process as given above does not contain the interactions of category (iii) and (iv) which simplifies the calculation considerably. Photon exchange diagrams of category (ii) are rather complicated to compute since they involve five point functions. It has been argued that this type of diagrams can be neglected with respect to the other ones[6]. In general this is based on the argument that these diagrams belong to the class of t-channel graphs. At large transverse momentum these graphs get suppressed because of a momentum mismatch appearing in the Feynman integrals for the box diagrams. This is corroborated by a calculation of corrections to electron electron scattering by Tsai[7]. However, one has to bear in mind that here the smallness of the box contributions is due to the scattering of two identical particles where a large cancellation can occur between the u and t channel graphs. Moreover it is certainly not applicable to processes where total cross-sections can be calculated since here the integration is also extended to small momentum transfers. The argument that at large momentum transfer the box graphs are suppressed seems to be invalidated by a calculation of Mo and Tsai[8] for electron proton scattering. Here the box graphs contribute a considerable part to the total correction. However one has to be careful with its interpretation since only the sum of the virtual and soft bremsstrahlung were considered with the hard photon radiation contributions left out. Therefore it is not clear whether diagrams of category (ii) will give an important contribution under experimental conditions that are typical for two photon physics. Considering however that the five-point functions form a gauge invariant set in their own and involve a higher amount of complexity we will

leave them for a later publication and concentrate ourselves on the peripheral contributions of category (i). Therefore we will only study the radiative corrections to the $e^{\pm}e^{\pm}\gamma$ vertices in the reaction $e^+e^- \to e^+e^-X$ where X is a pointlike pseudoscalar particle. In chapter II we will show how one can add virtual and real photon graphs in such a way that a fast and accurate numerical computation of the total and differential cross-sections is achieved. This will be an improvement on the standard way where first the virtual and soft bremsstrahlung contributions are computed. Their sum depends on the cut-off parameter in the photon energy Δ, where Δ is taken to be smaller than the mass of the electron. If $\Delta \ll m$ one is allowed to interchange angular and momentum integrations in the final state so that the total sum of virtual and soft bremsstrahlung graphs only depends on the momentum transfers of one of the two incoming leptons. If one later adds the hard photon contributions the total result will depend on Δ and one only recovers the correct answer if Δ is taken to be very small. This is awkward since it involves much computer time so that this procedure is unsuitable to make an event generator. Therefore we will develop a method which leads to a result which is independent of Δ so that an arbitrary value for Δ can be substituted leading to a considerable gain in computation time. In chapter III we calculate the hadronic contributions to the vacuum polarizations. The results for the total and differential cross-sections are discussed in chapter IV.

II. The Method

Let us consider the reaction $e^+e^- \to e^+e^-X$ (fig. 1) where X stands for a pointlike pseudoscalar with arbitrary mass M. We will assume that the interaction of X with the two photons can be described by the following phenomenological Lagrangian:

$$L_{int}(x) = \frac{1}{4} g \, \phi_X(x) \, \varepsilon^{\mu\nu\rho\sigma} \, F_{\mu\nu}(x) \, F_{\rho\sigma}(x) \, . \qquad (1)$$

The first order radiative corrections to the above process are given by the real photon graphs of fig. 2 and the virtual photon graphs of fig. 3. As mentioned in

the introduction we will not consider the one photon exchange graphs of figs 3i-ℓ. Since these graphs cancel the infra-red divergences of the interference between the graphs 2a,b and 2c,d we will omit those too. It can now be noted that the graphs 2a,b and 3a-c,g lead to the same result as the sets 2c,d and 3d-f,h. Therefore we have to calculate the first mentioned graphs only. Total cross-section results can then be found by doubling while $d\sigma/dq^2$ can be obtained by adding $d\sigma/dq_1^2$ and $d\sigma/dq_2^2$.

The matrix element corresponding to the real photon process (for the momentum assignment see fig. 4a) is given by:

$$|M|^2 = F^{\mu\nu} W_{\mu\nu} . \tag{2}$$

Here $W_{\mu\nu}$ denotes the structure tensor corresponding to the virtual photon Compton scattering process $(-q_1) + p_1 \to p_8 + p_9$ (fig. 4b). The latter process describes the real photon radiation at the upper vertex of the graphs in figure 4a whereas the remaining part of these graphs is represented by $F^{\mu\nu}$.

$W^R_{\mu\nu}$ (the R stands for radiative) is decomposed in the invariant structure functions W_i^R as follows:

$$W^R_{\mu\nu} = \sum_{i=1}^{4} T^{(i)}_{\mu\nu} \; W_i^R \tag{3}$$

where the $T_{\mu\nu}^{(i)}$ are given by

$$T^{(1)}_{\mu\nu} = 2q_1^2 \left(g_{\mu\nu} - \frac{q_{1\mu} q_{1\nu}}{q_1^2}\right) \tag{4a}$$

$$T^{(2)}_{\mu\nu} = 8 r_{1\mu} r_{1\nu} \tag{4b}$$

$$T^{(3)}_{\mu\nu} = 8 r_{9\mu} r_{9\nu} \tag{4c}$$

$$T^{(4)}_{\mu\nu} = 4\left(r_{1\mu} r_{9\nu} + r_{1\nu} r_{9\mu}\right) \tag{4d}$$

with

$$r_{i\mu} = p_{i\mu} - \frac{p_i \cdot q_1}{q_1^2}\, q_{1\mu} \,. \tag{5}$$

From the above Compton process we infer:

$$W_1^R = \frac{1}{q_1^2}\left(4m^2 q_1^2 - 2(s_3-m^2)(t-m^2)\right)\left(\frac{1}{(s_3-m^2)^2} + \frac{1}{(t-m^2)^2}\right) + \frac{4(s_3+t-q_1^2)}{(s_3-m^2)(t-m^2)} \tag{6a}$$

$$W_2^R = 4m^2\left\{\frac{1}{(s_3-m^2)^2} + \frac{1}{(t-m^2)^2}\right\} + \frac{4(2m^2-q_1^2)}{(s_3-m^2)(t-m^2)} \tag{6b}$$

$$W_3^R = \frac{4m^2}{(t-m^2)^2} - \frac{2q_1^2}{(s_3-m^2)(t-m^2)} \tag{6c}$$

$$W_4^R = -\frac{8m^2}{(t-m^2)^2} - \frac{4(2m^2-q_1^2)}{(s_3-m^2)(t-m^2)} \tag{6d}$$

where $s_3 = (p_8 + p_9)^2$ and $t = (p_8 + q_1)^2 = (p_1 - p_9)^2$. Using the above, the matrix element without its coupling constants can now be cast into the form[9]:

$$\begin{aligned}|M^R|^2 = \frac{-1}{(q_1^2 q_2^2)}\big[&2q_1^2 W_1 \varepsilon^{q_1 q_2 \mu\lambda}\varepsilon_{q_1 q_2 \nu\lambda} + 8W_2 \varepsilon^{p_1 q_1 \mu q_2}\varepsilon_{p_1 q_1 \nu q_2} \\ &+ 8W_3 \varepsilon^{p_9 q_1 \mu q_2}\varepsilon_{p_9 q_1 \nu q_2} + 4W_4 \varepsilon^{p_9 q_1 \mu q_2}\varepsilon_{p_1 q_1 \nu q_2} \\ &+ 4W_4\, \varepsilon^{p_1 q_1 \mu q_2}\varepsilon_{p_9 q_1 \nu q_2}\big]\,(2q_2^2\, g_\mu{}^\nu + 8p_{2\mu}p_2{}^\nu)\end{aligned} \tag{7}$$

The ε stands for the Levi-Civita tensor and we have adopted the notation $\varepsilon^{p\nu\rho\sigma} = \varepsilon^{\mu\nu\rho\sigma}p_\mu$ where p is a four vector. The numerical evaluation of most of the terms in eq. 7 is discussed in ref. 9.

The matrix element of the virtual photon graphs (fig. 3a,b,c) is denoted by:

$$|M^V|^2 = F^{\mu\nu} W^V_{\mu\nu} \tag{8}$$

where $W^V_{\mu\nu}$ is the structure tensor corresponding to the virtual photon corrections at the upper vertex. $W^V_{\mu\nu}$ can be expressed in the virtual photon structure functions

$$W^V_{\mu\nu} = \sum_{i=1}^{2} T^{(i)}_{\mu\nu} W^V_i \tag{9}$$

For future purposes we shall split the virtual contributions into two parts, one due to the vertex (fig. 3b) and self energy corrections (fig. 3a,c) and the other one due to the vacuum polarization graph of fig. 3g. In the latter one there are besides electron and muon also hadronic contributions taken into account.

In first order of QED the contribution of the vertex and self energy corrections is given by the interference between graph 1 and the graphs 3a,b,c. The corresponding structure functions become:

$$\begin{aligned} W_1^{V_1} &= 2\left[F_1^{V_1}(q_1^2) - F_2^{V_1}(q_1^2)\right] \\ W_2^{V_1} &= 2 F_1^{V_1}(q_1^2) \end{aligned} \tag{10}$$

where the $F_1^V(q_1^2)$ are the well-known Pauli-Dirac form factors which are given by[10]:

$$F_1^{V_1}(q_1^2) = \frac{\alpha}{2\pi}\left[\frac{2+3y}{\sqrt{y(1+y)}}\ln\tau - \frac{1+2y}{\sqrt{y(1+y)}}\left\{-2\ln\frac{\lambda}{m}\ln\tau + \ln^2\tau\right.\right.$$

$$\left.\left. - Li_2\left(\frac{2\sqrt{y}}{\tau}\right) + \frac{1}{2}Li_2\left(\frac{4\sqrt{y(1+y)}}{\tau^2}\right)\right\}\left\{-2\ln\frac{\lambda}{m} - 2\right]\right. \tag{11}$$

$$F_2^{V_1}(q_i^2) = \frac{\alpha}{2\pi} \frac{\ln \tau}{\sqrt{y(1+y)}}$$

Here we have defined $y = -q_1^2/4m^2$ and $\tau = \sqrt{y} + \sqrt{1+y}$. Furthermore we have introduced a photon mass λ in order to regulate the infra-red singularities. The structure functions corresponding to the vacuum polarization contribution are equal to:

$$W_i^{V_2} = 2 F^{V_2}(q_i^2) \tag{12}$$

with

$$F^{V_2}(q_i^2) = \frac{\alpha}{3\pi}\left[-\frac{5}{3} + \frac{1}{y} + \frac{\sqrt{1+y}}{y\sqrt{y}}(2y-1)\ln\tau\right] \tag{13}$$

From eqs (1), (8) and (9) we can obtain the matrix element corresponding to the virtual contributions. It is given by:

$$|M^V|^2 = \frac{g^2}{(q_1^2 q_2^2)^2}\left[-64\,\epsilon^{p_1 q_1 p_2 q_2}\epsilon_{p_1 q_1 p_2 q_2} W_2^V - 16 q_1^2 \epsilon^{\mu q_1 p_2 q_2}\epsilon_{\mu q_1 p_2 q_2} W_1^V \right. \tag{14}$$

$$\left. - 16 q_2^2 \epsilon^{p_1 q_1 \mu q_2}\epsilon_{p_1 q_1 \mu q_2} W_2^V + 8 q_1^2 q_2^2 \{(q_1 q_2)^2 - q_1^2 q_2^2\} W_1^V\right]$$

The first product of Levi-Civita tensors is equal to Δ_4 where Δ_4 is the Gram determinant of the system. The latter is always negative in the physical region. Since the remaining scalars $\epsilon^{\mu q_1 p_2 q_2}\epsilon_{\mu q_1 p_2 q_2}$, $\epsilon^{p_1 q_1 \mu q_2}\epsilon_{p_1 q_1 \mu q_2}$ and $(q_1 q_2)^2 - q_1^2 q_2^2$ are always positive in the physical region we conclude that if all $W_i > 0$ all terms in the matrix element (14) are positive. From this and eqs (10)-(13) we infer that the vertex and self energy corrections lead to a negative contribution whereas the vacuum polarization leads to a positive contribution in eq. (14).

Now we have given the matrix elements corresponding to the various processes we

are able to calculate cross-sections, which will be denoted by

$$\sigma = \int F^{\mu\nu} W_{\mu\nu} \, dPS \tag{15}$$

where dPS stands for the momenta over which we integrate. In this section we will not worry about the experimental criteria for the difference between the soft and the hard radiation. Therefore we will integrate over the photon momentum writing $dPS = ds_3 \, d\Omega^{CM} \, dPS$. Here s_3 is defined as in eq. 6, Ω^{CM} is the solid angle indicating the direction of the photon in the centre of mass system of s_3 and dPS represents the rest of the integrations. Since $F^{\mu\nu}$ does not depend on Ω^{CM} one can write for the real photon cross-section:

$$\sigma^R = \int_{m^2}^{s_3^{max}} ds_3 \int F^{\mu\nu} \left\{ \int d\Omega^{CM} W^R_{\mu\nu} \right\} d\overline{PS} \tag{16}$$

The new structure tensor $\bar{W}^R_{\mu\nu} = \int d\Omega^{CM} \, W^R_{\mu\nu}$ depends on the two momenta p_1 and q_1 only, so it takes the form:

$$\overline{W}^R_{\mu\nu} = \sum_{i=1}^{2} T^{(i)}_{\mu\nu} \, \overline{W}^R_i \tag{17}$$

The $\bar{W}_i^R$ are nothing but the structure functions corresponding to the integrated forward virtual Compton process in fig. 4b. They can be obtained from the eqs (3) and (4) by using the following projection operators:

$$P_{1\mu\nu} = \frac{g_{\mu\nu}}{4q_1^2} + \frac{p_{1\mu}p_{1\nu}}{\lambda_1}$$

$$P_{2\mu\nu} = \frac{q_1^2}{4\lambda_1} \left\{ g_{\mu\nu} + \frac{12q_1^2}{\lambda_1} p_{1\mu}p_{1\nu} \right\} \tag{18}$$

with $\lambda_1 = \lambda(s_3, q_1^2, m^2) = s_3^2 + (q_1^2)^2 + m^4 - 2s_3q_1^2 - 2s_3m^2 - 2m^2q_1^2$. In this way the $\bar{W}_i^R$ become:

$$\overline{W}_i^R = \int d\Omega \, P_i^{\mu\nu} \, W^R_{\mu\nu} \tag{19}$$

After a straightforward calculation we get:

$$\bar{W}_1^R(s_3, q_1^2) = \frac{1}{4q_1^2} C + \frac{1}{\lambda_1} D$$

$$W_2^R(s_3, q_1^2) = \frac{q_1^2}{4\lambda_1}\left\{C + \frac{12q_1^2}{\lambda_1} D\right\} \tag{20}$$

The quantities C and D are given by:

$$C = \frac{2\alpha}{\pi}\left[\left\{-\frac{s_3^2 + s_3 q_1^2 + 4 s_3 m^2 + m^2 q_1^2 - m^4}{2 s_3^2}\right.\right. \tag{21a}$$

$$\left.\left. + \frac{2q_1^2 - s_3 + 5m^2}{\lambda_1^{1/2}} \ln x\right\} - \frac{q_1^2 + 2m^2}{s_3 - m^2}\left\{4 + \frac{2(q_1^2 - 2m^2)}{\lambda_1^{1/2}} \ln x\right\}\right]$$

$$D = \frac{\alpha}{2\pi}\left[\left\{\frac{s_3^2 - q_1^2 s_3 - 16 m^2 s_3 + m^2 q_1^2 - m^4}{s_3}\right.\right. \tag{21b}$$

$$\left.\left. + \frac{2m^2(3s_3 - 6q_1^2 + 13m^2)}{\lambda_1^{1/2}} \ln x\right\} + \frac{2m^2(q_1^2 - 4m^2)}{s_3 - m^2}\left\{4 + \frac{2(q_1^2 - 2m^2)}{\lambda_1^{1/2}} \ln x\right\}\right]$$

with

$$x = \frac{s_3 + m^2 - q_1^2 + \lambda_1^{1/2}}{s_3 + m^2 - q_1^2 - \lambda_1^{1/2}} = \frac{(s_3 + m^2 - q_1^2 + \lambda_1^{1/2})^2}{4 m^2 s_3} \tag{22}$$

Insertion of these expressions for $\bar{W}_1^R$ and $\bar{W}_2^R$ into eq. (16) reveals that the cross-section σ^R becomes infra-red divergent which is due to the pole terms in $(s_3 - m^2)^{-1}$ in eqs (21a) and (21b). However, since the virtual photon cross-section σ^V which is defined by

$$\sigma^V = \int F^{\mu\nu} W_{\mu\nu}^V \, d\bar{P}S \tag{23}$$

is also infra-red divergent (see eq. (11)) both divergences are cancelled in the sum according to the Bloch Nordsieck theorem[11,12]. The cancellation of the infra-red divergence is achieved by introducing the photon mass regulator λ in $\bar{W}_i^R$ (eqs (19) and (16)) in the phase space integral. The s_3 integral runs then from $(m+\lambda)^2$ to s_3^{max}. Evaluation of σ^R then produces a $\ell n\lambda$ term which is cancelled by the corresponding one appearing in σ^V. However, because of the many integration variables in dPS (at least 4) σ^R has to be evaluated numerically. This leads to numerical inaccuracies in the determination of the $\ell n\lambda$ and the non-logarithmic terms. Therefore we split σ^R in two parts, one containing the infra-red divergence, while the other one is infra-red finite. The infra-red divergent part is then partially computed analytically in such a way that it can be added to σ^V. The finite part of σ^R can then safely be evaluated numerically. Below we will present several different ways in which one can add σ^R to σ^V.

Let us split σ^R into a soft photon part σ^S containing the infra-red divergence and a hard photon part σ^H which is infra-red finite. They are defined by:

$$\sigma^S = \int_{(m+\lambda)^2}^{\Delta} ds_3 \int F^{\mu\nu} \bar{W}^S_{\mu\nu}(\lambda)\, d\overline{PS} \tag{24a}$$

$$\sigma^H = \int_{\Delta}^{s_3^{max}} ds_3 \int F^{\mu\nu} \bar{W}^R_{\mu\nu}\, d\overline{PS} \tag{24b}$$

where Δ is chosen arbitrarily. $\bar{W}^S_{\mu\nu}(\lambda)$ represents the structure tensors $\bar{W}_i^R$ in which the infra-red regulator λ has been introduced. The next step is to interchange in eq. (24a) the integration over s_3 and the contraction with $F^{\mu\nu}$:

$$\bar{\sigma}^S = \int F^{\mu\nu} \left\{ \int_{(m+\lambda)^2}^{\Delta} ds_3 \bar{W}^S_{\mu\nu}(\lambda) \right\} d\overline{PS} \tag{25}$$

This introduces an error because once the contraction with $F^{\mu\nu}$ is performed new terms in s_3 will appear. If this is done after integration over s_3 the best that can be done is to put s_3 in these new terms equal to m^2. Therefore $\bar{\sigma}^S$ differs from σ^S in the following way:

$$\bar{\sigma}^S - \sigma^S = \sum_{i=1}^{\infty} a_i \left(\frac{\Delta - m^2}{m^2}\right)^i \tag{26}$$

assuming that in all finite terms the limit $\lambda \to 0$ has been taken. The transition from eq. (24a) to eq. (25) has also caused the integration order between s_3 and the rest of phase space to be changed. In the integration boundaries of dPS we will implement this by setting $s_3 = m^2$ and this approximation also contributes to the coefficients a_i in equation (26). The expression for σ^V is

$$\sigma^V = \int_{m^2}^{s_3^{max}} ds_3 \int d\overline{PS}\; F^{\mu\nu} W^V_{\mu\nu}\, \delta(s_3 - m^2) \tag{27}$$

making the dPS integration in σ^V equal to the dPS integration in $\bar{\sigma}^S$. Due to the above procedure the total cross-section $\sigma = \sigma^V + \bar{\sigma}^S + \bar{\sigma}^H$ becomes Δ dependent, and we will only obtain the exact total cross section in the limit $\Delta \to m^2$. We will see later that it is important to have the approach to the limiting cross section as smooth as possible. Therefore we have investigated several methods ending up with a procedure by which the total cross-section does not depend on Δ anymore. These methods are presented below.

(I). The first method is the standard one which is very often used in the literature. Here we use $\Delta - m^2 \ll m^2$ so that $\bar{\sigma}^S$ is virtually equal to σ^S because the omitted terms are negligible. The calculation of $\bar{\sigma}^S$ is then the same as if we had applied the eikonal approximation to the real photon matrix element. $\bar{W}_{\mu\nu}(\lambda)$ becomes:

$$\bar{W}^S_{\mu\nu}(\lambda) = \sum_{i=1}^{2} T^{(i)}_{\mu\nu}\, W^S_i(\lambda) \tag{28}$$

in which W_i^S is given by

$$W^S_i(\lambda) = \delta(s_3 - m^2)\, B \tag{29}$$

with

$$B = \frac{\alpha}{3\pi^2} \int_0^{\omega} \frac{d^3\vec{p}_g}{\sqrt{|\vec{p}_g|^2+\lambda^2}} \left\{ \frac{p_{1\mu}}{p_1 p_g} - \frac{p_{8\mu}}{p_8 p_g} \right\}^2 \tag{30}$$

and $\omega = \frac{\Delta - m^2}{2m} << m$

A straightforward calculation provides us with the answer[12]:

$$B = \frac{\alpha}{\pi}\left[1 - 2\ln\frac{\Delta-m^2}{m\lambda} - \frac{1+2y}{\sqrt{y(1+y)}}\left\{-2\ln\tau\ln\frac{\Delta-m^2}{m\lambda} + 2\ln^2\tau + \frac{1}{2}Li_2\left(\frac{4\sqrt{y(1+y)}}{\tau^2}\right) - \ln\tau\right\}\right] \tag{31}$$

Addition of W_i^S to W_i^V cancels the infra-red divergence so that we obtain:

$$W_1^{V+S} = W_1^V + W_1^S = \frac{\alpha}{\pi}\left[\frac{1+3y}{\sqrt{y(1+y)}}\ln\tau - \frac{1+2y}{\sqrt{y(1+y)}}\left\{-2\ln\frac{\Delta-m^2}{m^2}\ln\tau + 3\ln^2\tau - \ln\tau + Li_2\left(\frac{4\sqrt{y(1+y)}}{\tau^2}\right) - Li_2\left(\frac{2\sqrt{y}}{\tau}\right)\right\} - 1 - 2\ln\frac{\Delta-m^2}{m^2}\right] \tag{32a}$$

$$W_2^{V+S} = W_2^V + W_2^S = \frac{\alpha}{\pi}\left[\frac{2+3y}{\sqrt{y(1+y)}}\ln\tau - \frac{1+2y}{\sqrt{y(1+y)}}\left\{-2\ln\frac{\Delta-m^2}{m^2}\ln\tau + 3\ln^2\tau - \ln\tau + Li_2\left(\frac{4\sqrt{y(1+y)}}{\tau^2}\right) - Li_2\left(\frac{2\sqrt{y}}{\tau}\right)\right\} - 1 - 2\ln\frac{\Delta-m^2}{m^2}\right] \tag{32b}$$

In fig. 5 we show the total cross-section $\sigma_t = \sigma_t^V + \bar{\sigma}_t^S + \sigma_t^H$ as a function of $\sqrt{\Delta}$ (curve I). We observe that the slope of the curve is very steep which implies that σ_t becomes already very Δ dependent for values of $\Delta - m^2$ of the order of m^2. From this we infer that the real total cross-section is only approached if $\Delta - m^2/m^2$ is chosen to be very small. However the determination of the total cross-section for small Δ will cost us much computer time. This is due to the fact that for a fixed amount of computer time one obtains for each of the terms

in σ_t a fixed relative accuracy. For smaller values of $\Delta-m^2/m^2$ the individual terms in σ_t have a larger absolute value and thus a larger error causing the error in σ_t to be larger. To obtain the same absolute error in σ_t as for larger values of Δ one therefore needs more computer time.

It will by now be clear that it is important to have an accurate value for σ_t for as large a value of Δ as possible. This implies that we must find a different W_1^S which will lead to a σ which slowly varies with Δ.

(II). In the first method we made two approximations. The first one was the interchange of the integration over s_3 with the contraction with $F_{\mu\nu}$ and the rest of the integrals. The second one was the eikonal approximation where all photon momenta are neglected in the matrix element. The second method consists of dropping the eikonal approximation. For this we have to proceed as follows. We split the integral in eq. (25) into two parts:

$$W^S_{\mu\nu}(\lambda) = \int_{(m+\lambda)^2}^{\Delta} ds_3 \, \overline{W}^R_{\mu\nu}(\lambda)$$
$$= \int_{(m+\lambda)^2}^{(m+\omega)^2} ds_3 \, \overline{W}^R_{\mu\nu}(\lambda) + \int_{(m+\omega)^2}^{\Delta} ds_3 \, \overline{W}^R_{\mu\nu}(0) \qquad (33)$$

Since the infra-red divergence is only present in the first term of equation (33) we can take the limit $\lambda \to 0$ in the second term. If we take now $\omega \ll m$ we can again apply the eikonal approximation to $\bar{W}^R_{\mu\nu}(\lambda)$ so that the first integral leads to the expressions (28) and (29) with Δ replaced by $(m+\omega)^2$. Using the expressions of eq. (20) for $\bar{W}^R_{\mu\nu}(0)$ the computation of the second integral in eq. (33) becomes straightforward but tedious. Adding $W^S_{\mu\nu}(\lambda)$ to $W^V_{\mu\nu}$ we obtain two structure functions like in eq. (32). They are:

$$W_1^{V+S} = \frac{\alpha}{\pi}\left[\frac{1+4y+3y^2+3x+2x^2+5xy}{4y\,w(x)}\ln z - \frac{x}{4y} - \frac{x(1+4y)}{4y(1+4x)}\right. \tag{34a}$$

$$+ \frac{3+8y}{8y}\ln(1+4x) - 1 - 2\ln 4x + \frac{2y^2-2y-1}{y\sqrt{y(1+y)}}\ln\tau$$

$$\left. + \frac{1-y}{2y} I_1 - \frac{1+2y}{\sqrt{y(1+y)}} I_2\right]$$

$$W_2^{V+S} = \frac{\alpha}{\pi}\left[\left\{\frac{1+2y+x}{2w(x)} + \frac{y(1+y)^2+xy(1+y)}{4(w(x))^3}\right\}\ln z\right.$$

$$- \frac{y(1+y)(1+5y)+xy(1+3y)}{(1+4y)(w(x))^2} + \frac{y}{(1+4x)(1+4y)} \tag{34b}$$

$$\left. + \frac{3}{2}\ln(1+4x) - 2\ln 4x - \frac{\ln\tau}{2\sqrt{y(1+y)}} - \frac{1+2y}{2\sqrt{y(1+y)}} I_2\right]$$

where we have defined the quantities x, y, W(x), τ and z by:

$$x = \frac{\Delta - m^2}{4m^2} \quad ; \quad y = -\frac{q_i^2}{4m^2} \quad ; \quad w(x) = \sqrt{y + (x+y)^2} \tag{35}$$

$$\tau = \sqrt{y} + \sqrt{1+y} \qquad z = \frac{x+y+1/2+w(x)}{x+y+1/2-w(x)}$$

The quantities I_1 and I_2 are given by:

$$I_1 = Li_2\left(\frac{2y}{w(x)+x+y}\right) - Li_2\left(\frac{w(x)+x+y}{w(x)+x+y+1/2}\right) + 2\ln^2\tau \tag{36}$$

$$- \tfrac{1}{2}\ln^2(2w(x)+2x+2y+1)$$

$$I_2 = \frac{1}{2}\ln 2 \ln\left\{\frac{(w(x)+x+y+1/2)^2}{2x(w(x)+x+y)}\right\} - \frac{1}{4}\ln^2\left\{\frac{w(x)+x+y}{w(x)+x-y}\right\}$$

$$-\frac{1}{2}\ln\left\{\frac{w(x)+x+y}{w(x)+x-y}\right\}\ln\left\{\frac{2x}{w(x)+w(0)+x}\right\} - \frac{1}{2}Li_2\left(\frac{w(x)-w(0)+x}{w(x)+x+y+1/2}\right)$$

$$+\frac{1}{2}Li_2\left(\frac{w(x)+w(0)+x}{w(x)+x+y+1/2}\right) - \frac{1}{2}Li_2\left(\frac{w(0)-y}{w(x)+x-y}\right) + \frac{1}{2}Li_2\left(\frac{w(0)+y}{w(x)+x+y}\right) \qquad (37)$$

$$-\frac{1}{2}Li_2\left(\frac{w(0)+y}{w(x)+w(0)+x}\right) + \frac{1}{2}Li_2\left(\frac{w(0)-y}{w(x)+w(0)+x}\right)$$

As far as the integration of equation (33) concerns the above formulae are exact in Δ. Using this method II we again computed the total cross-section $\sigma_t = \sigma^V + \bar{\sigma}^S + \sigma^H$ as a function of $\sqrt{\Delta}$ (see curve II in fig. 5). Comparison of the first two methods shows that we have achieved a slight improvement only. The second curve is a little bit less steep for small values of Δ but still the variation of σ_t as a function of Δ is too large, so we have to search for another method.

(III). As we have already mentioned earlier, the interchange of the integral over s_3 and the contraction with $F_{\mu\nu}$ is only correct if $\Delta - m^2 \ll m^2$. Bearing in mind that we used the above procedure only to cancel the infra-red divergence it is sufficient to interchange integration and contraction for the pole part of $\bar{W}^R_{\mu\nu}$ only. Therefore we split $\bar{W}^R_{\mu\nu}$ as follows:

$$\overline{W}^R_{\mu\nu} = \overline{W}^P_{\mu\nu} + \overline{W}^F_{\mu\nu} \qquad (38)$$

where

$$\overline{W}^P_{\mu\nu} = \sum_{i=1}^{2} T^{(i)}_{\mu\nu}\,\overline{W}^P_i \quad ; \quad \overline{W}^F_{\mu\nu} = \sum_{i=1}^{2} T^{(i)}_{\mu\nu}\,\overline{W}^F_i \qquad (39)$$

with:

$$\bar{W}_i^P = \frac{\alpha}{\pi}\frac{1}{s_3-m^2}\left[-2+\frac{1+2y}{\sqrt{y(1+y)}}\ln\tau\right] \qquad (s_3<\Delta)$$

$$= 0 \qquad (s_3>\Delta) \qquad (40)$$

$$\bar{W}_i^F = \bar{W}_i^R - \bar{W}_i^P \qquad (41)$$

This way, using eqs (20) and (21) to define the $\bar{W}_i^R$, the $\bar{W}_i^f$ are finite in s_3-m^2. Now we can split the soft photon cross-section σ^S as follows:

$$\sigma^S = \int_{(m+\lambda)^2}^{\Delta} ds_3 \int F^{\mu\nu}\,\bar{W}^S_{\mu\nu}(\lambda)\,d\bar{PS}$$

$$= \int d\bar{PS}\,F^{\mu\nu}\int_{(m+\lambda)^2}^{(m+\omega)^2} ds_3\,\bar{W}^S_{\mu\nu}(\lambda)$$

$$+ \int d\bar{PS}\,F^{\mu\nu}\int_{(m+\omega)^2}^{\Delta} ds_3\,\bar{W}^P_{\mu\nu} + \int_{m^2}^{\Delta} ds_3 \int d\bar{PS}\,F^{\mu\nu}\bar{W}^F_{\mu\nu} \qquad (42)$$

The interchange of contraction and integration is allowed in the first integral because $\omega<<m$. The only approximations are now made in the second integral. Remark also that the sum of the first two terms is equal to the $\bar{\sigma}^3$ which we obtained by using method I (eq. (32)). Therefore the difference $\sigma_t(\mathrm{III})-\sigma_t(\mathrm{I})$ is given by the last term in eq. (42). Comparing this last method with the former ones we observe that curve III (in fig. 5) has a much smaller slope than the former curves.

(IV). Once the only approximations that are made occur in the pole term it is possible to correct for the change in the order of integration. For this we write down the original integral (after the Ω integration) of the pole term:

$$\int_{(m+\omega)^2}^{\Delta} ds_3 \int \frac{ds_2\, dt_1\, dt_2\, ds_1}{\sqrt{-\Delta_4(s_3)}}\; F^{\mu\nu}\, \overline{W}^{p}_{\mu\nu} \tag{43}$$

In this form no approximations have been made yet. The notation is according to ref. 9 which means that

$$\begin{aligned} s_1 &= (p_3 + p_4)^2 \qquad & s_2 &= (p_4 + p_5)^2 \\ t_1 &= (p_1 - p_3)^2 \qquad & t_2 &= (p_2 - p_5)^2 \end{aligned} \tag{44}$$

and Δ_4 is the Gram determinant of the $2\to3$ reaction in which $s_3 = p_3^2 = (p_8 + p_9)^2$ is the mass squared of one of the outgoing particles. When the order of integration is changed the boundaries of the s_1, s_2, t_1, t_2 integrals take the values that they would have had for $s_3 = m^2$. The upper boundary of the s_3 integral could however become smaller than Δ depending on the values of s_2, t_1, t_2, and s_1. The necessary conditions are obtained by successive exchange of integrals. The exchange with s_2 gives:

$$\sqrt{s_3} < \sqrt{s} - \sqrt{s_2} \tag{45}$$

Then the exchange with t_1 gives the relation:

$$s_3 < \frac{-b + \sqrt{b^2 - 4m^2 c}}{2m^2} \tag{46}$$

with:

$$\begin{aligned} b &= (s - m^2)(s_2 - t_1) - m^2(s + s_2 + t_1) \\ c &= s t_1 (s + t_1 - s_2 - 2m^2) + m^2 s_2 (s_2 - s) + m^4 s \end{aligned} \tag{47}$$

The exchange with t_2 gives no restrictions on the value of s_3 and the final condition is due to the exchange with s_1:

$$s_3 < \frac{(-b'-d')}{2a'} \tag{48}$$

with:

$$a' = \frac{m^4 \lambda(t_2, m^2, m^2)}{16 \Delta_4(m^2)} = \frac{-m^4 t_2 (4m^2 - t_2)}{16 \Delta_4(m^2)} < 0$$

$$b' = \frac{-m^2}{\Delta_4(m^2)} \Big\{ p_2 q_2 \left(p_1 p_2 \, q_1 q_2 + p_1 q_2 \, p_2 q_1 - p_1 q_1 \, p_2 q_2 \right.$$

$$\left. - 2 p_1 p_2 \, p_2 q_1 + 2 m^2 \, p_1 q_1 \right) - m^2 \, p_1 q_2 \, q_1 q_2 \Big\} \tag{49}$$

$$d' = \frac{-m^2}{\Delta_4(m^2)} \left\{ \epsilon^{p_2 q_2 q_1 \mu} \epsilon_{p_2 q_2 q_1 \mu} \epsilon^{p_1 p_2 q_2 \nu} \epsilon_{r_1 p_2 q_2 \nu} \right\}^{1/2}$$

The real upper limit of the s_3 integral is the minimum of Δ and the three eqs (45), (46) and (48). This we will call Δ^-. The phase-space integral becomes now:

$$\int_{(m+\omega)^2}^{\Delta} ds_3 \int \frac{ds_2 dt_1 dt_2 ds_1}{\sqrt{-\Delta_4(s_3)}} = \int \frac{ds_2 dt_1 dt_2 ds_1}{\sqrt{-\Delta_4(m^2)}} \int_{(m+\omega)^2}^{\Delta^-} ds_3 \left[\frac{\Delta_4(m^2)}{\Delta_4(s_3)} \right]^{1/2} \tag{50}$$

The resulting integral over s_3 can be done analytically because only the $(s_3 - m^2)^{-1}$ part of the matrix element is included in the integrant. After a change of variable the integral becomes:

$$\int_{\frac{2m\omega+\omega^2}{m^2}}^{\frac{\Delta^- - m^2}{m^2}} \frac{du}{u} \frac{1}{\sqrt{1+b'u+a'u^2}} \tag{51}$$

where we defined $u = (s_3 - m^2)/m^2$. The final expression becomes

$$- \ln \left\{ \frac{\frac{1}{2} b'u + 1 + \sqrt{1+b'u+a'u^2}}{u} \right\} \Bigg|_{\frac{2m\omega+\omega^2}{m^2}}^{\frac{\Delta^- - m^2}{m^2}} \tag{52}$$

It should be noted that when the upper bound is substituted the $\sqrt{1+b'u+a'u^2}$ becomes zero if Δ^- finds its origin in eq. (48). Substitution of the lower boundary gives again the $\ln(\omega/m)$ term that cancels against the corresponding term from the first integral in eq. (42). The complete correction to the s_3 integral is obtained by subtracting the originally used du/u integral for the pole term in eq. (42) obtaining thereby:

$$W_i^I = \frac{\alpha}{\pi} \left\{ -2 + \frac{1+2y}{\sqrt{y(1+y)}} \ln \tau \right\} \cdot I_3 \tag{53}$$

with

$$I_3 = - \ln \left\{ \frac{1 + \frac{1}{2} u b' + \sqrt{1+b'u+a'u^2}}{u} \right\} \Bigg|_{u = \frac{\Delta^- - m^2}{m^2}} + \ln 2 - \ln \frac{\Delta - m^2}{m^2} \tag{54}$$

This correction turns out to be relatively small so we have not given a curve IV in fig. 5 as it would be quite close to curve III.

(V). At this point there is only one approximation left, being the interchange of the s_3 integral and the contraction of $F^{\mu\nu}$ with $\bar{W}^P_{\mu\nu}$. The error that is made in this contraction has one more power of (s_3-m^2) than the complete contraction so this error is finite. To correct for it we only have to evaluate $F^{\mu\nu}T_{\mu\nu}^{(i)}$ in powers of $s_3 - m^2$. The constant term was used together with method IV already. The higher order terms can be used with the original kinematics by rewriting eq. (42) once more

$$\sigma^S = \int d\bar{PS}\, F^{\mu\nu} \int_{(m+\lambda)^2}^{(m+w)^2} ds_3\, \bar{W}^S_{\mu\nu}(\lambda)$$

$$+ \int d\bar{PS} \int_{(m+w)^2}^{\Delta^-} ds_3 \sum_{i=1}^{2} \frac{F^{\mu\nu} T^{(i)}_{\mu\nu}(s_3=m^2)}{\sqrt{1+b'u+a'u^2}}\, \bar{W}_i^P$$

$$+ \int_{m^2}^{\Delta} ds_3 \int d\bar{PS} \sum_{i=1}^{2} \left\{ F^{\mu\nu} T^{(i)}_{\mu\nu} - F^{\mu\nu} T^{(i)}_{\mu\nu}(s_3=m^2) \right\} \bar{W}_i^P \qquad (55)$$

$$+ \int_{m^2}^{\Delta} ds_3 \int d\bar{PS}\, F^{\mu\nu} \bar{W}^F_{\mu\nu}$$

The contraction of $F^{\mu\nu}$ with $T_{\mu\nu}^{(1)}$ does not depend on s_3 so it does not contribute to the third integral. The contribution from $T_{\mu\nu}^{(2)}$ to the third integral is

$$F^{\mu\nu}T^{(2)}_{\mu\nu} - F^{\mu\nu}T^{(2)}_{\mu\nu}(s_3=m^2) = \frac{1}{t_1^2 t_2^2}\Big[16 t_2 m^2 (s_3-m^2)^2$$

$$- (s_3-m^2)\Big\{ 32 t_1 t_2 m^2 - 64 t_2\, p_1\cdot p_2\, p_2\cdot q_1 - 16(t_2+4m^2) p_1\cdot q_2\, q_1\cdot q_2 \qquad (56)$$

$$+ 64 (p_1\cdot p_2\, q_1\cdot q_2 + p_1\cdot q_2\, p_2\cdot q_1)\, p_2\cdot q_2 \Big\}\Big]$$

The sum of method III and the results of IV and V is represented by curve V in fig. 5. This curve is completely independent of $\sqrt{\Delta}$ as it should be because we have removed all approximations. We checked this even for $\sqrt{\Delta} = 10\ m_e$ and still got the same result. This makes the calculations much easier because from now on we can calculate cross-sections for one rather large value of Δ (typically $\sqrt{\Delta} \approx 5m_e$) rather than having to use various values of Δ and study the limit $\Delta \to 0$.

Using a very large value for Δ serves no purpose because then the interplay between the eikonal approximation and its correction terms (mainly method III) starts causing big cancellations resulting in bigger errors in the answers. Finally we show in appendix A how the eqs (13), (32a) and (32b) are evaluated in the region of small q_1^2. In this region these equations become numerically unstable.

III. Hadronic contribution to the vacuum polarization

In the previous chapter we have given the contribution to the vacuum polarization (fig. 3g,h) from the electrons only, see eq. (13). In addition we can now also include heavier leptons like the muon and the tau which contributions are given by the same formula in eq. (13) where m_e is replaced by m_μ and m_τ respectively. In practice it turns out that only the muonic contribution is important since the vacuum polarization decreases rapidly if the lepton mass gets larger.

Besides the leptonic we have also to include hadronic contributions to the vacuum polarizations. Like in the case of the leptons the hadronic part of the vacuum polarization is included by modifying the photon propagator in the following way (see also ref. 13)

$$\frac{g_{\mu\nu}}{q^2} \longrightarrow \frac{g_{\mu\nu}}{q^2}\left(1 - F_h^{V_2}(q^2)\right) \tag{57}$$

where $F_h^{V_2}(q^2)$ is defined by

$$\mathrm{Re}\, F_h^{V_2}(q^2) = \frac{q^2}{4\pi^2\alpha}\int_{s_0}^{\infty} ds' \, \frac{\sigma(s')}{s'-q^2} \tag{58}$$

and $\sigma(s')$ denotes the total cross section of $e^+e^- \to$ hadrons and s_0 is the threshold which value is equal to $4m_\pi^2$. Note further that $F_h^{V_2}(q^2) < 0$ so that we obtain a positive contribution to the radiative correction of the two photon process. Following the analysis in ref. 13 $\sigma(s')$ can be written as a sum of vector meson resonances below a certain value $s=s_1$. Above this value the total cross-section is approximated by the continuum described by the process $e^+e^- \to q\bar{q}$ in the quark parton model. For $s<s_1$ $\sigma(s')$ is given by the narrow width approximation.

$$\sigma(s') = \sum_V \frac{12\pi \Gamma_V \Gamma_{l,V}}{(s'-m_V^2)^2 + m_V^2 \Gamma_V^2} \tag{59}$$

where V stands for the following vector mesons ρ, ω, ϕ, ρ', ψ and ψ'. Γ_V, $\Gamma_{l,V}$ and m_V denote the full width, the leptonic width and the mass of the vector mesons respectively. On the first sight the narrow width formula seems to be a crude approximation to describe the broad vector mesons ρ and ρ'. However, we have checked that a more realistic prescription for $\sigma(s')$ like e.g. the Gounaris Sakurai parametrization[14] of the Breit Wigner form yields a result which almost does not differ from the narrow width approximation. Furthermore we have to bear in mind that the ρ' parameters are not very well known. Moreover the parameters describing the other vector mesons have also some uncertainties so that we feel that the above formula eq. (59) gives a good description of the hadronic vacuum polarization which serves our purposes. The same also holds for our omission of the ω-ρ interference. For $s>s_1$ $\sigma(s')$ is given by

$$\sigma(s') = R(s_1) \frac{4\pi\alpha^2}{3s'} \tag{60}$$

where $R(s_1)$ denotes the sum over all quark changes multiplied by the colour factor, i.e. $R(s_1) = 3 \sum_{i=1}^{6} q_i^2 = 5$ (6 flavours). Inserting eq. (59) and (60) into eq. (58) we obtain

$$\mathrm{Re}\, F_h^{V_2}(q^2) = \frac{3q^2}{\alpha}\sum_V \frac{\Gamma_{e,V}}{m_V}\,\frac{m_V^2 - q^2}{(q^2 - m_V^2)^2 + m_V^2\Gamma_V^2} - \frac{\alpha}{3\pi} R(s_1)\,\mathrm{Ln}\left|\frac{s_1 - q^2}{s_1}\right| \qquad (61)$$

In the derivation of eq. (61) we have taken s_1 large enough so that for $s > s_1$ the Breit Wigner formula in eq. (59) can be identified with zero. In the evaluations of the dispersion integral this implies that we can take the limit $s_1 \to \infty$. Therefore the first term on the right-hand side of eq. (61) is independent of s_1.

IV. Results

Using the method described in chapter II we will first show the results for the corrections to the total cross-section. In figure 5 we have presented σ_t^c/σ_t for beam energies of 15 GeV (PETRA, PEP) and 50 GeV (LEP). Here σ_t^c represents the α^5 cross-section due to the vertex and self-energy corrections on the $e^+e^-\gamma$ vertex including the leptonic (e,μ) and hadronic part of the vacuum polarization whereas σ_t stands for the lowest order α^4 cross-sections. From fig. 6 we infer that the corrections are small. The bulk of the radiative correction can be attributed to the leptonic and hadronic part of the vacuum polarization whereas the vertex and bremsstrahlung graphs almost cancel each other. Further we have checked that there is no noticeable difference between scalar and pseudoscalar production in two photon reactions. Our results at 15 GeV agree with those of Defrise in ref. [6] provided we omit the muonic and hadronic part of the vacuum polarization in our calculations. Since total cross-sections of more than 100 nb are often reduced to a few pb inside the acceptance of a detector we can conclude that they are not the most interesting observables in two photon physics. Therefore it is better to study the differential distribution $d\sigma/dq^2$. Here $d\sigma/dq^2$ is obtained by taking the sum of $d\sigma/dq_1^2$ and $d\sigma/dq_2^2$ where q_1^2 is the q^2 on the side of the corrected vertex (including the vacuum polarization) and q_2^2 is the q^2 on the away side. The differential cross-section is shown in fig. 7 and fig. 8 for beam energies of 15 GeV and 50 GeV respectively. The dashed lines in figures 7

and 8 represent the contribution from the vacuum polarization to $d\sigma/dq_1^2$ only. Like in the case of the total cross-section we observe that the bulk of the radiative corrections can be attributed to the vacuum polarization whereas the remainder is considerably smaller and negative. From the figures we infer that in the physically interesting range ($1\ \mathrm{GeV}^2 < |q^2| < 100\ \mathrm{GeV}^2$) the corrections are of the order of a few percent only. This is 3-5% for PETRA or PEP energies and 5-6% for LEP. The turn-over of the curve near $|q^2| = 100$ GeV in fig. 7 can be traced back to a reduction in phasespace. It appears that near the boundary of phasespace the bremsstrahlung graphs get suppressed stronger than the virtual photon contributions since the latter contain a particle less in the the final state. One of the features of the measurements of radiative corrections is that they can be influenced by the properties of the detector. If one would like to measure $d\sigma/dt$ where t is the momentum transfer between the in- and outgoing electron (positron) it is necessary to measure the proper value of t for each event. This is not always possible due to the presence of an unobservable radiated photon. This photon would either have too little energy so that it is undetectable or stay in the beam pipe. In the first case this is not so serious since it would not affect the value of q^2 for the event too much. However in the latter case this is annoying because this leads in the reconstruction of q^2 to a much larger value than the event really has. This can be easily shown as follows. The theoretical value for q^2 reads

$$q^2 = (p^e_{in} - p^e_{out} - p^\gamma)^2 \simeq -2\,p^e_{in}\,p^e_{out} - 2\,p^e_{in}\,p^\gamma + 2\,p^e_{out}\,p^\gamma \qquad (62)$$

where p^e_{in}, p^e_{out} and p^γ denote the in- and outgoing momenta of the electron and photon respectively. The observed value for q^2 is equal to

$$q^2_{observed} \simeq -2\,p^e_{in}\,p^e_{out} \qquad (63)$$

Notice that in eq. (62) and (63) we have neglected the masses of the electron (positron). If the outgoing photon is parallel to p^e_{in} the product $p^e_{in} \cdot p^\gamma$ becomes very small and the error in $q^2_{observed}$ is $2p^e_{out} \cdot p^\gamma$, a (potentially large) positive number. This implies that q^2_{obs} is more negative than q^2 causing a migration of

events with a small value of $|q^2|$ to observed events with a large value of $|q^2_{obs}|$. The result is an increase in $d\sigma/dq^2$ at large values of $|q^2|$. We have measured this effect for various detector geometries. For a LEP detector which can observe photons with an energy larger than 200 MeV and with an angle down to 20 mrad the corrections to q^2_{obs} are less than 0.1%. At lower beam energies these corrections are somewhat larger and become at best 1% for the maximum value of $|q^2|$ at a beam energy of 15 GeV. We conclude that these corrections are not very important. This may seem to contradict some findings in ep and up[8] collisions where there are regions in phasespace in which they are very large (30% or more). However, here these corrections are found at large values of ν or y in $d\sigma/d\nu$ or $d\sigma/dy$ respectively and not in $d\sigma/dq^2$. For the definitions of ν and y see ref. [15]. Eventually this will also become important for two photon physics if one wants to measure the photon structure function near y=1 or at very large $|q^2|$ for a fixed value of x. Here y and x are defined as $y = q_2 \cdot q_1 / q_2 \cdot p^e_{in}$ and $x = -q_1^2 / 2q_1 \cdot q_2$ where p^e_{in} is the momentum of the incoming electron (positron) and q_1, q_2 are the momenta of the highly virtual and almost real photon respectively. However, it will take a long time before one has enough data to observe the above effect. Our viewpoint is that for the time being these effects will be small in two photon experiments.

Conclusions

The radiative corrections to pseudoscalar production in the two photon reaction $e^+e^- \to e^+e^-X$ are of the order of 1 to 2% for the total cross-section. For the differential cross-sections they are larger and they become about 5% at large $|q^2|$. It is not expected that a change in spin of particle X will appreciably alter the above results. If we take a scalar instead of a pseudoscalar particle we do not find any noticeable change in the percentage of the radiative corrections. This indicates that the corrections to the process $e^+e^- \to e^+e^- \mu^+\mu^-$ will show the same order of magnitude as found above provided one integrates over the final state of the muon pair (see ref. [6]). If one also wants to observe the muon pair the average value for $|q^2|$ will increase which implies that the radiative

corrections become larger than in the former case. Finally we want to remark that all the above conclusions hold if one ignores diagrams which involve the five point functions, fig. 3i-l (category 2). The amount of their contribution can for the moment only be guessed.

We want to thank K.J.F. Gaemers, J. Smith and P. Duinker for having useful discussions.

Appendix A

When evaluating eq. (32) one has to pay some attention to numerical instabilities. In the expression (32) there are terms that behave individually like $y^{-\frac{1}{2}} = \sqrt{4m^2/-q_1^2}$. The full expression can however be shown to behave as a power expansion in y in which the lowest order term is proportional to y. This means that one and a half powers of y get cancelled between the various terms. Considering that $-q_1^2/4m^2$ has a minimum value of less than 10^{-10} when the beam energy is in the PETRA, PEP or LEP range, great care is needed. We have therefore made some power expansions which are used whenever $-q_1^2/4m^2 < 0.1$. The first one is:

$$F_2^{V_1}(q_1^2) = \frac{\alpha}{2\pi} \frac{\ln\tau}{\sqrt{y(1+y)}} = \frac{\alpha}{2\pi} \sum_{n=0}^{\infty} \frac{1}{1+y} \frac{z^n}{(2n+1)} \qquad \text{(A1)}$$

with $z = \frac{y}{y+1}$

The coefficient of $\ln \Delta - m^2/m^2$ in eq. (32) can be written as

$$B = 2\left[\frac{1+2y}{\sqrt{y(1+y)}} \ln\tau - 1\right] = 2\sum_{n=1}^{\infty} \frac{4n}{4n^2-1} z^n \qquad \text{(A2)}$$

After these preliminaries W_2^{V+S} in equation (32b) can be written as

$$W_2^{V+S} = \frac{\alpha}{\pi}\left\{\sum_{n=1}^{\infty} a_n z^n + B \ln\frac{\Delta - m^2}{m^2}\right\} \qquad \text{(A3)}$$

The coefficients a_n can be easily computed by using the algebraic manipulation program SCHOONSCHIP. The first 10 values of a_n are given in table 1. An analogous expansion for W_1^{V+S} can be obtained from W_2^{V+S} (A3) and $F_2^{V_1}$ (A1). The expansion of F^{V_2} in eq. (13) is given by

$$F^{V_2} = \sum_{n=1}^{\infty} \frac{4(n+2)}{(2n+1)(2n+3)} z^n \qquad \text{(A4)}$$

References

[1] E. Witten, Nucl. Phys. B120 (1977) 189
W.A. Bardeen and A.J. Buras, Phys. Rev. D20 (1979) 166
D.W. Duke and J.W. Owens, Phys. Rev. D22 (1980) 2280

[2] "Two Photon Physics", W.A. Bardeen, published in the Proceedings of the 1981 International Symposium on Lepton and Photon Interactions at High Energies, Editor W. Pfeil.

[3] Ch. Berger et al., Phys. Lett. 94B (1980) 254
K. Brandelik et al., Zeitschrift für Physik C10 (1980) 117
Ch. Berger et al., DESY preprint 82-004

[4] See the talks presented by P. Kessler and J. Smith which are published in "$\gamma\gamma$ collisions", Proceedings Amiens 1980, Edited by G. Cochard and P. Kessler, Springer Verlag Berlin.

[5] G. Cochard and S. Ong in "Radiative corrections to $\gamma\gamma$ processes in e^+e^-, e^-e^-, e^+e^+ collision rings", published in "$\gamma\gamma$ collisions", Proceedings Amiens 1980, Edited by G. Cochard and P. Kessler, Springer Verlag Berlin.
M. Defrise, S. Ong, J. Silva and C. Carimalo, Phys. Rev. D23 (1981) 663.
Y. Srivastava, "Radiative corrections for photon photon scattering", published in the fourth International Colloquium on Photon Photon Interactions 1981, Edited by G.W. London World Scientific Singapore.

[6] M. Defrise in "Contribution to the Analysis of Photon Photon collisions in electron-positron storage rings", Ph.D. Thesis 1982; Vrije Universiteit Brussel, Faculteit der Wetenschappen, Brussels, Belgium.

[7] Y.S. Tsai, Phys. Rev. 120 (1960) 269

[8] Y.S. Tsai, Phys. Rev. 122 (1960) 1898
L.W. Mo and Y.S. Tsai, Rev. Mod. Phys. 41 (1969) 205

[9] J.A.M. Vermaseren, preprint NIKHEF-H/82-15 to be published in Nucl. Phys. B.

[10] R. Barbieri, J.A. Mignaco and E. Remiddi, Nuovo Cim. 11A (1972) 824

[11] F. Bloch and A. Nordsieck, Phys. Rev. 52 (1932) 54; ibid. 52 (1932) 59

[12] D.R. Yennie, S.C. Frautschi and H. Suura, Ann. of Phys. 13 (1961) 379

[13] F.A. Berends and G.J. Komen, Phys. Lett. 63B (1976) 432

[14] G.J. Gounaris and J.J. Sakurai, Phys. Rev. Lett. 21 (1968) 244

[15] P.V. Landshof and H. Osborne in "Electromagnetic interactions of hadrons" Volume 2, Edited by A. Donnachie and G. Shaw in Nuclear Physics Monographs, Plenum Press New York.

Table captions:

Table 1: The coefficients a_n in the expansion of eq. (A3).

Figure captions

Fig. 1. Lowest-order graph of the process $e^+e^- \to e^+e^- X$.

Fig. 2. First-order real photon corrections to the process $e^+e^- \to e^+e^- X$.

Fig. 3. First-order virtual photon corrections to the process $e^+e^- \to e^+e^- X$.

Fig. 4. (a) real photon corrections to the upper $ee\gamma$ vertex of fig. 1,
(b) virtual compton scattering process $(-q_1) + p_1 \to p_8 + p_9$.

Fig. 5. First-order corrections to the total cross-section of $e^+e^- \to e^+e^-X$ computed via methods I: (1), II: (2), III: (3) and IV: (4) mentioned in chapter II. M=0.15 GeV, E=15 GeV.

Fig. 6. First-order correction to the total cross-section as function of the pseudo-scalar mass M,
(1) E=50 GeV
(2) E=15 GeV

Fig. 7. First-order correction to the differential cross-section $d\sigma/dq^2$ as function of $|q^2|$ for E=15 GeV, M=0.5 GeV;
(1) contribution from $d\sigma/dq_1^2$,
(2) contribution from $d\sigma/dq_2^2$,
--- contribution from the vacuum polarization (fig. 3g) to $d\sigma/dq_1^2$.

Fig. 8. First-order correction to the differential cross-section $d\sigma/dq_2$ as function of $|q|^2$ for E=50 GeV, M=0.5 GeV;

(1) contribution from $d\sigma/dq_1^2$,

(2) contribution from $d\sigma/dq_2^2$,

--- contribution from the vacuum polarization (fig. 3g) to $d\sigma/dq_1^2$.

* * *

Table 1

n	a_n
1	-11/9
2	-593/225
3	-2703/1225
4	-37273/19845
5	-112421/68607
6	-1043179/715715
7	-36691/27885
8	-5214299/4339335
9	-578317599/522166645
10	-398045983/387017631

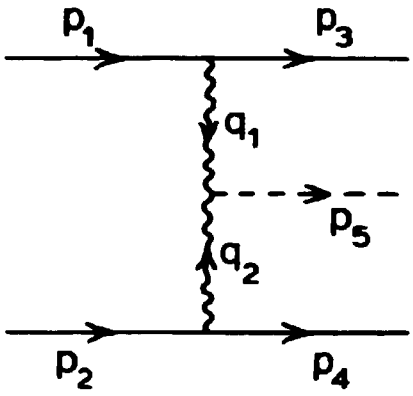

Fig. 1

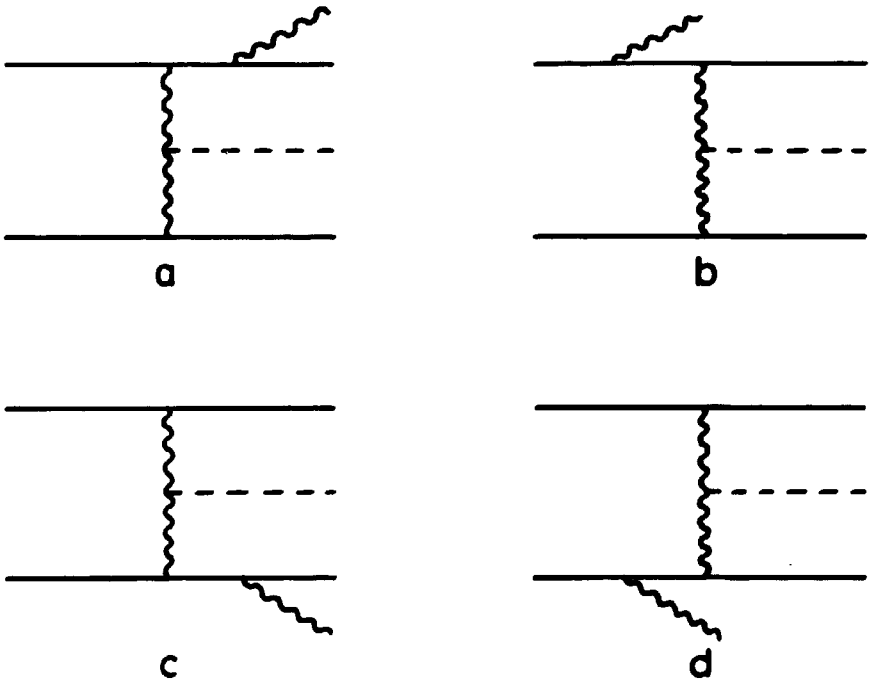

Fig. 2

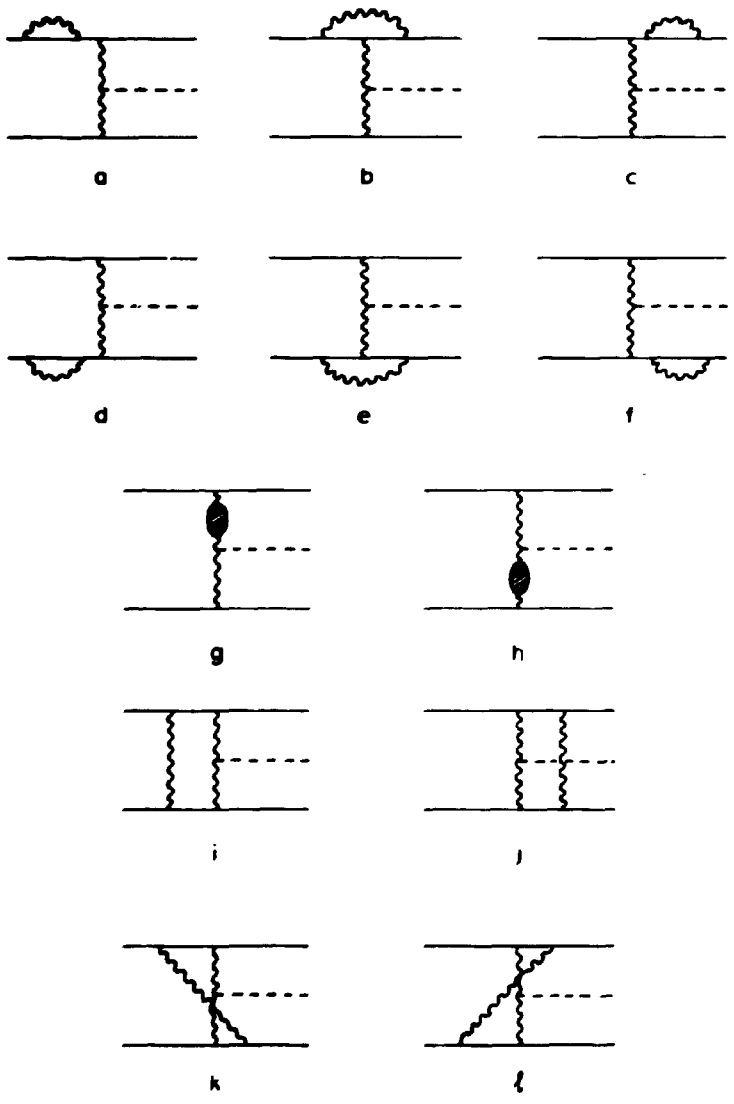

Fig 3

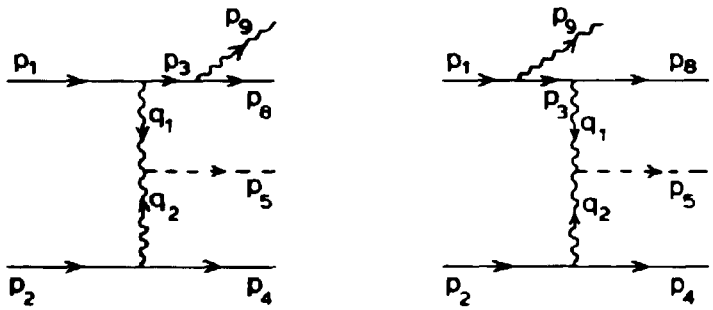
p9
p1
p3
p8
q1
q2
p5
p2
p4
p9
p1
p8
p3
q1
q2
p5
p2
p4

a

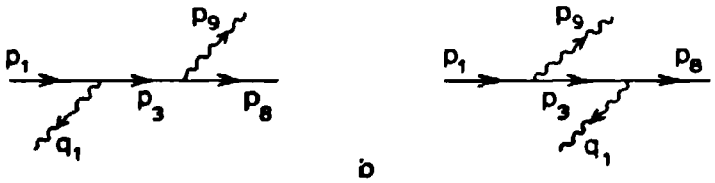
p9
p1
p3
p8
q1
p9
p1
p8
p3
q1

b

Fig. 4

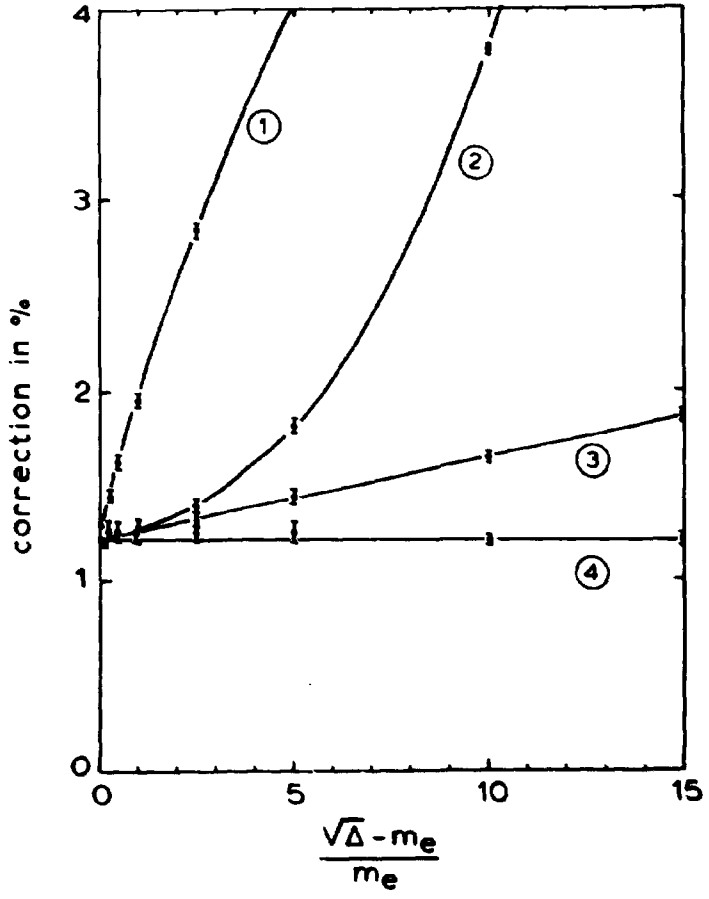
correction in %
0
1
2
3
4
0
5
10
15
①
②
③
④
$\frac{\sqrt{\Delta} - m_e}{m_e}$

Fig 5

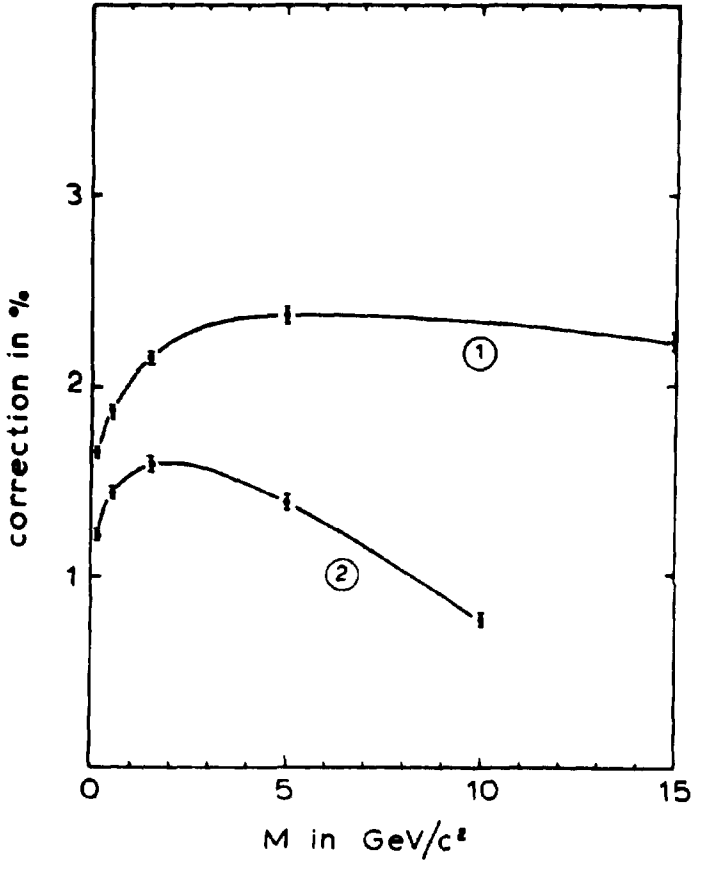
correction in %
1
2
3
0
5
10
15
①
②
M in GeV/c²

Fig 6

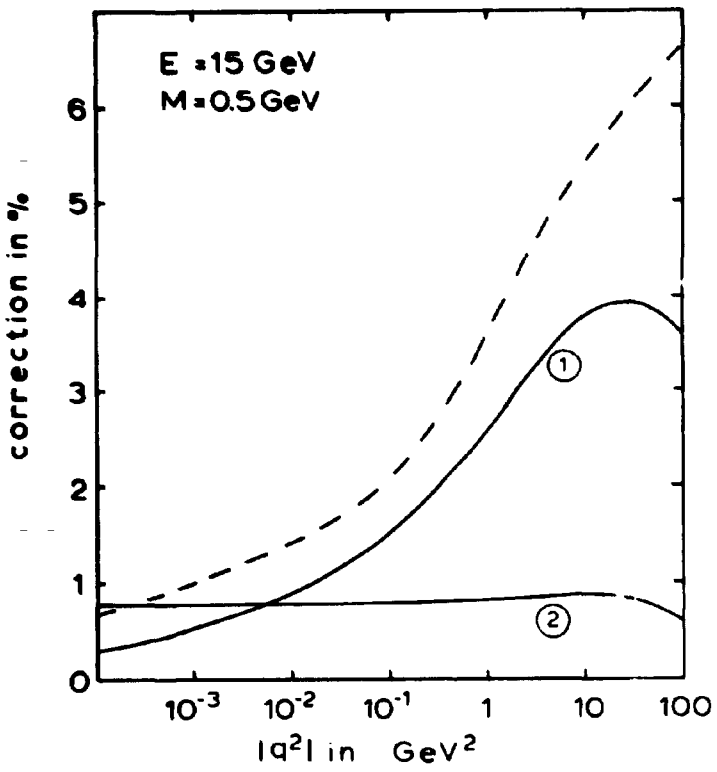
E =15 GeV
M=0.5 GeV
correction in %
0
1
2
3
4
5
6
①
②
10^{-3}
10^{-2}
10^{-1}
1
10
100
$|q^2|$ in GeV^2

Fig 7

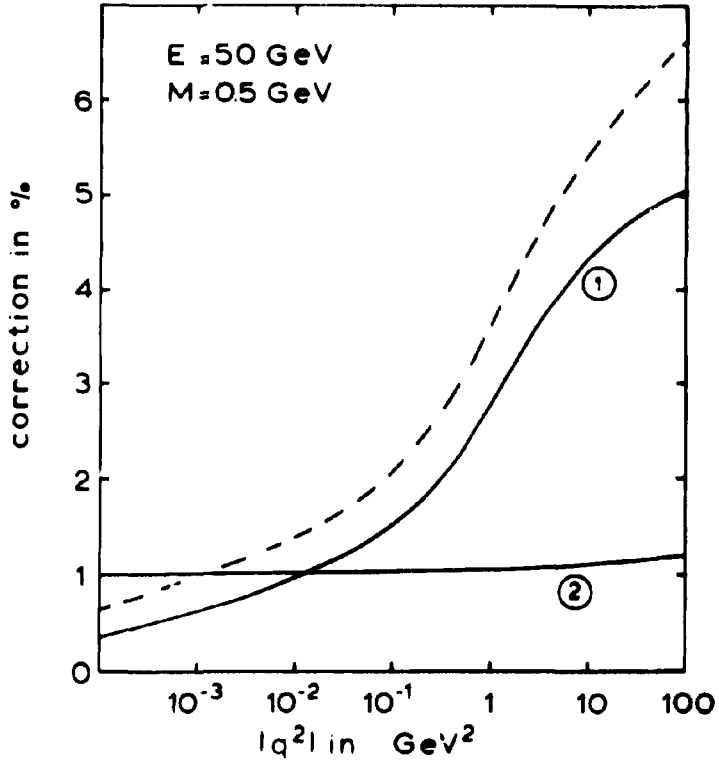
E =50 GeV
M=0.5 GeV
correction in %
0
1
2
3
4
5
6
①
②
10^{-3}
10^{-2}
10^{-1}
1
10
100
$|q^2|$ in GeV^2

Fig 8